HHS Public Access

Author manuscript

Ecotoxicol Environ Saf. Author manuscript; available in PMC 2022 December 18.

Published in final edited form as:

Ecotoxicol Environ Saf. 2022 December 01; 247: 114253. doi:10.1016/j.ecoenv.2022.114253.

Deficiency of interleukin-6 receptor ameliorates $PM_{2.5}$ exposure-induced pulmonary dysfunction and inflammation but not abnormalities in glucose homeostasis

Renzhen Peng[a,1], **Wenhui Yang**[a,1], **Wenpu Shao**[a], **Bin Pan**[a], **Yaning Zhu**[b], **Yubin Zhang**[a], **Haidong Kan**[a], **Yanyi Xu**[a,*], **Zhekang Ying**[c,**]

[a] Department of Environmental Health, School of Public Health, Fudan University, Shanghai, China

[b] Department of Pathology, The Affiliated Huaian No.1 People's Hospital of Nanjing Medical University, Huaian, China

[c] Department of Medicine Cardiology Division, University of Maryland School of Medicine, Baltimore, MD, USA

Abstract

Background: Ambient fine particulate matter ($PM_{2.5}$) exposure increases local and systemic interleukin-6 (IL-6). However, the pathogenic role of IL-6 signalling following $PM_{2.5}$ exposure, particularly in the development of pulmonary dysfunction and abnormal glucose homeostasis, has hardly been investigated.

Results: In the study, IL-6 receptor (IL-6R)-deficient ($IL\text{-}6R^{-/-}$) and wildtype littermate ($IL\text{-}6R^{+/+}$) mice were exposed to concentrated ambient $PM_{2.5}$ (CAP) or filtered air (FA), and their pulmonary and metabolic responses to these exposures were analyzed. Our results demonstrated that IL-6R deficiency markedly alleviated $PM_{2.5}$ exposure-induced increases in lung inflammatory markers including the inflammation score of histological analysis, the number of macrophages in bronchoalveolar lavage fluid (BALF), and mRNA expressions of TNFα, IL-1β and IL-6 and abnormalities in lung function test. However, IL-6R deficiency did not reduce the hepatic insulin resistance nor systemic glucose intolerance and insulin resistance induced by $PM_{2.5}$ exposure.

*Correspondence to: School of Public Health, Fudan University 130 Dong'an Rd, Shanghai 200032, China. yanyi_xu@fudan.edu.cn (Y. Xu). **Correspondence to: School of Medicine, University of Maryland 20 Penn St. HSFII S022, Baltimore, MD 21201, USA. yingzhekang@hotmail.com, zying@medicine.umaryland.edu (Z. Ying).

[1]These authors contribute equally to this work

Author's contributions

Renzhen Peng: Investigation, Methodology, Formal analysis and Wring – original draft; **Wenhui Yang:** Methodology, Formal analysis and Investigation; **Wenpu Shao:** Methodology and Investigation; **Bin Pan:** Investigation; **Yaning Zhu:** Formal analysis; **Yubin Zhang:** Investigation and Resources; **Haidong Kan:** Writing – review & editing and Conceptualization; **Yanyi Xu:** Supervision, Conceptualization, Funding acqusition and Writing – review & editing; **Zhekang Ying:** Supervision, Conceptualization, Funding acqusition and Writing – review & editing.

Declaration of Competing Interest

The authors declare that they have no known competing financial interests or personal relationships that could have appeared to influence the work reported in this paper.

Appendix A. Supporting information

Supplementary data associated with this article can be found in the online version at doi:10.1016/j.ecoenv.2022.114253.

Conclusion: Our findings support the crucial role of IL-6 signalling in the development of pulmonary inflammation and dysfunction due to $PM_{2.5}$ exposure but question the putative central role of pulmonary inflammation for the extra-pulmonary dysfunctions following $PM_{2.5}$ exposure, providing a deep mechanistic insight into the pathogenesis caused by $PM_{2.5}$ exposure.

Keywords

$PM_{2.5}$; IL-6R; Inflammation; Pulmonary dysfunction; Glucose homeostasis

1. Introduction

Fine particulate matters ($PM_{2.5}$) exposure is correlated with various adverse health effects including pulmonary dysfunction, non-alcoholic fatty liver disease, abnormal glucose metabolism and so forth.(EPA, 2020) Numerous studies have demonstrated that $PM_{2.5}$ exposure provokes marked pulmonary inflammation, which is widely considered to be responsible for not only $PM_{2.5}$ exposure-induced pulmonary dysfunction (Shamsollahi et al., 2021) but also various extra-pulmonary inflammations and dysfunctions.(Arias-Pérez et al., 2020) Interlukin-6 (IL-6) is one of the best known pulmonary (Hamanaka and Mutlu, 2018) and circulating (Mutlu et al., 2007) inflammatory markers that are up-regulated by exposure to $PM_{2.5}$. Previous studies also revealed that IL-6, a pleiotropic four-helix-bundle cytokine, (Giraldez et al., 2021) was the primary culprit for the pulmonary inflammation,(Mutlu et al., 2007) accelerated thrombosis, (Mutlu et al., 2007) and ovarian dysfunction caused by $PM_{2.5}$ exposure.(Zhou et al., 2020) However, the role of IL-6 signaling in the development of other adverse health effects due to $PM_{2.5}$ exposure, e.g., abnormal glucose homeostasis, has hardly been investigated. Both epidemiological and toxicological studies have shown that IL-6 signaling pathway is implicated in the pathophysiology of type 2 diabetes (T2D).(Akbari and Hassan-Zadeh, 2018; Aparicio-Siegmund et al., 2019) For instance, the elevated level of IL-6 in circulation has been considered as an independent predictor of T2D, (Rehman et al., 2017) and IL-6 signaling pathway is found to be involved in the development of insulin resistance and β-cell dysfunction.(Huang et al., 2022; Marasco et al., 2018) Furthermore, increasing studies have shown that effect of IL-6 signaling in inflammation and glucose homeostasis is context-dependent.(Giraldez et al., 2021) It may be pro-inflammatory and pro-diabetic in some contexts but anti-inflammatory and anti-diabetic in other contexts. (Giraldez et al., 2021) As such, there is obviously an urgent need of pinpointing the role of IL-6 signaling in $PM_{2.5}$ exposure-induced abnormal glucose homeostasis.

On membrane-bound IL-6 receptor (mbIL-6R) expressing cells, IL-6 may directly bind to this mbIL-6R and subsequently recruit gp130 to form a signaling transduction complex. (Giraldez et al., 2021) This IL-6 signaling is referred to the classic signaling of IL-6 and generally believed to be anti-inflammatory and anti-diabetic. (Giraldez et al., 2021) IL-6 may also bind to the soluble IL-6R (sIL-6R) to form an agonistic complex and subsequently activate gp130.(Giraldez et al., 2021) This IL-6 signaling is referred to the trans-signaling of IL-6 and is believed to be pro-inflammatory and pro-diabetic. All of these clearly demonstrate that IL-6R not only is essential for IL-6 signaling but also largely determines the effect of IL-6 signaling in glucose homeostasis and inflammation.(Brenachot et al., 2017; Hunter and Jones, 2015; Narazaki and Kishimoto, 2018) The generation and

validation of IL-6R knockout mice has made it possible to use this model to investigate the role of IL-6 signaling in inflammation and abnormal glucose homeostasis.(McFarland-Mancini et al., 2010) Therefore, in the present study, we exposed IL-6R-deficient (IL-6R$^{-/-}$) and wildtype littermate (IL-6R$^{+/+}$) mice to CAP and thoroughly assessed their metabolic and inflammatory responses.

2. Materials and methods

2.1. Animals, whole-body CAP exposure, and $PM_{2.5}$ characterization

All the animals in this study were treated humanely with regards for suffering alleviation. The mouse strain C57BL/6 N-Il6ra^{em1cyagen} was obtained from Cyagen Biosciences. All the IL-6R-deficient (IL-6R$^{-/-}$) and littermate control mice (IL-6R$^{+/+}$) were genotyped when they were 1-week-old before the whole-body CAP exposure. This study was approved by the Institutional Animal Care and Use Committee (IACUC) at Fudan University (Approval number 2020JS-002).

A 26-week whole-body CAP exposure (from November 2020 to April 2021) was conducted using a versatile aerosol concentration enrichment system (VACES).(Xu et al., 2019) In brief, 6-week-old male IL-6R-deficient (IL-6R$^{-/-}$) and littermate control (IL-6R$^{+/+}$) mice were randomly grouped and then consecutively exposed to filtered air (FA) or CAP (n = 11–12/group). The Whatman HEPA-VENT filter (Thomas Scientific, USA) is used to remove the $PM_{2.5}$ in FA chamber (retention rate of 99.97% for all particles < 0.3 μm in size). The exposure was performed for 5 days/week and 8 h/day (no exposure on weekends). $PM_{2.5}$ samples in the CAP and FA chambers and the ambient air were collected every week by using PTFE (Polytetrafluoroethylene) membrane filters (SKC Ltd, UK) at the outlet of the chambers, and their compositions were analyzed by Wavelength Dispersive X-ray fluorescence spectrometry (WD-XFS) using RIX 3000 (Rigaku, USA). In brief, a rhodium X-ray tube was used at 50 kV and 50 mA, and the characteristic X-rays were measured under vacuum (3–7 Pa) with coarse slit and field diaphragm diameter of 30 mm. The quantitative analysis standards of all the detected elements were set using the inorganic elemental standard filters from US Micro Matter company, and the relative errors for measurement of the quality control samples were within 10%.

The mice were housed in a filtration system (Model OMCIF-V, Airclean, China) when not exposed to CAP or FA. During the experimental period, mice were kept at room temperature (20–25 °C) on a 12-h light/dark cycle with relative humidity of 40–70% and standard food and water ad lib.

2.2. Intraperitoneal glucose tolerance test (IPGTT)

After 18 weeks of FA/CAP exposure, mice (24 weeks old) were fasted for 16 h before IPGTT test. Firstly, the tail vein blood was collected and the basal glucose level was assessed by an automatic glucose meter (Roche Diagnostics). Then glucose was intraperitoneally injected to the mice (2 g/kg of body weight). 15, 30, 60 and 120 min after glucose injection, the blood glucose levels were measured as described above.

2.3. Insulin tolerance test (ITT)

After 19 weeks of FA/CAP exposure, mice (25 weeks old) were fasted for 4 h before ITT test. Firstly, the tail vein blood was collected and the basal glucose level was assessed by an automatic glucose meter (Roche Diagnostics). Then insulin was intraperitoneally injected to the mice (0.5 U/kg of body weight). 15, 30, 60 and 120 min after insulin injection, the blood glucose levels were measured accordingly.

2.4. Lung function test

The lung function was assessed on the day next to the last FA/CAP exposure by the AniRes2005 Lung Function System (Version 3.5, Bestlab Hi-Tech Co.). In brief, mice were anesthetized using pentobarbital sodium (50 mg/kg of body weight), tracheally intubated, and connected to a ventilator that is computer-controlled. The respiratory rate and ratio of expiration to inspiration durations were set at 90/min and 1.5:1, respectively. All data were then recorded by the system automatically and measured as described previously. (Xiang et al., 2019; Yue et al., 2017; Zheng et al., 2020) A port connected with a pressure transducer was used to estimate the pressure changes in the plethysmographic chamber. Parameters including forced vital capacity (FVC), forced expiratory volume in 0.1 s ($FEV_{0.1}$), ratio of $FEV_{0.1}$ to FVC, resistance of expiration (R_E), resistance of lung (R_L) and respiratory dynamic compliance (C_{dyn}) were determined as changes of airway function.

2.5. Bronchoalveolar lavage fluid (BALF) and tissue harvest

After fasted overnight, mice were intraperitoneally injected with insulin (10 U/kg of body weight, to assess the insulin-induced Akt phosphorylation of insulin sensitive tissues such as liver. After 20 min, mice were euthanized and their blood samples were collected from the orbital venous plexus. After cannulating the mouse trachea, the right primary bronchus was closed off by a ligation. BALF was collected by instilling and withdrawing sterile PBS supplied with ethylenediaminetetraacetic acid (EDTA) (0.1 mM) via the intratracheal tube for three times (approximately 1.5 ml BALF in total). Cytospin slides were prepared with Cytospin 3™ (Shandon) and stained with Giemsa. Numbers of neutrophils, lymphocytes, eosinophils, basophil, and monocytes/macrophages were estimated by a pathologist who is blinded to the grouping. The total cell number in BALF was assessed with a hemocytometer. After harvesting BALF, half of the lung tissues were fixed with 4% paraformaldehyde at a pressure of 50–55 cm H_2O, and the others were snap frozen in liquid nitrogen for further analysis. Other tissues including liver, epididymal fat, hypothalamus, brown adipose tissue, heart, spleen, pancreas, kidney, perirenal fat, subcutaneous fat, skeletal muscle, testis and epididymis were also harvested and weighted.

2.6. Real-time RT-PCR

Trizol reagent (Invitrogen) was used to extract and purify total RNA. The quality and quantity of extracted RNA was estimated by Nanodrop. After reversely transcribing the RNA into cDNA with High Capacity cDNA Reverse Transcription Kit (Applied Biosystems™), real-time RT-PCR was conducted on a 7500 Real-time PCR System (Applied Biosystems™) using the SYBR qPCR Master Mix (Vazyme). $2^{-\Delta Ct}$ were calculated as the

relative expression levels of the target genes. The primers information were given on Table S1 (GAPDH was used as the housekeeping gene).

2.7. Histological analysis

To assess lung inflammation, the lung block was embedded in paraffin, cut into 5-μm sections, and stained with hematoxylin and eosin (H&E). Images covering all 3 consecutive sections were obtained using Olympus IX73 inverted microscope and assessed according to the scoring standards of pulmonary inflammation as listed on Table 1. To perform histological analysis on liver, a part of the liver tissue was fixed in 4% paraformaldehyde for 24 h at 4 °C. The liver tissue was then embedded in paraffin, cut into 5-μm sections, and subjected to H&E (assessment of vacuolation) or Masson's trichrome staining (assessment of fibrosis). Another part of liver tissue was frozen in optimal cutting temperature compound (OCT), cut into 5-μm sections, and stained with Oil red O (assessment of lipid deposition). Images covering all 3 consecutive sections were obtained using Olympus IX73 inverted microscope and assessed by a pathologist who is blind to the grouping using ImageJ (version 1.53c).

2.8. Western blotting

Western blotting was conducted using standard techniques with primary antibodies: mouse-anti-AKT (Beyotime Biotechnology), rabbit anti-phospho-AKT (Cell Signaling), and mouse-anti-β-actin (Sigma). Signals were assessed by an enhanced chemiluminescence detection reagent (Biosharp, China) and quantitated by densitometry (ImageQuant Las 500, GE Healthcare).

2.9. Statistical analysis

All the data were presented as mean ± SEM when not specified otherwise. The area under curve (AUC) of the IPGTT and ITT results were estimated by GraphPad Prism Software (version 8). Statistical analyses were performed using two-way ANOVA followed by Bonferroni adjustment or student's *t* test using the GraphPad Prism Software (version 8). The significance level was set at $p < 0.05$.

3. Results

3.1. IL-6R deficiency alleviates pulmonary dysfunction induced by $PM_{2.5}$ exposure

The experimental scheme was demonstrated in Fig. 1A. The average concentrations of $PM_{2.5}$ over the whole experimental period in the ambient air as well as the FA and CAP chambers were 43.1 ± 23.4, 0.221 ± 0.832, and 225 ± 112 μg/m^3, respectively. Considering that the exposure was conducted for 5 days/week and 8 h/day, and all the mice were housed in a filtration system during the unexposed time, the time-weighted average $PM_{2.5}$ exposure levels of CAP- or FA-exposed mice were 53.6 and 0.0526 μg/m^3, respectively. The $PM_{2.5}$ level in CAP group was much higher than 35 μg/m^3, which is the national ambient air quality standard of China, (Xie et al., 2015)but was quite common in heavily polluted cities such as Handan, China. (Zhang et al., 2020) As demonstrated in Table 2, due to the detection limit and the quantification limit, some of the elements in ambient, FA and CAP chambers were not detected. For all the detected elements, their concentrations in CAP chamber

were markedly higher than those in ambient, and their fractions were comparable, evincing that our VACES enriched $PM_{2.5}$ in ambient without altering its chemical composition. In addition, the high levels of Si and S reflected the heavy transportation and construction environment on campus.(Karagulian et al., 2015).

Since lung is the best-known target organ of inhaled $PM_{2.5}$, we used spirometry to assess whether deficiency of IL-6R influences $PM_{2.5}$ exposure-induced pulmonary dysfunction. Fig. 1B–D show that CAP exposure significantly decreased $FEV_{0.1}$ and FVC, but increased $FEV_{0.1}$/FVC in wildtype mice, strongly suggesting that CAP exposure primarily provoked restrictive lung disease in these mice. This provocation of restrictive lung disease was corroborated by the decrease in lung dynamic compliance (C_{dyn}) (Fig. 1G). Notably, CAP exposure also significantly increased R_L and R_E in wildtype mice (Fig. 1E–F), manifesting that CAP exposure indeed provoked both restrictive and obstructive lung diseases in wildtype mice. Except the decrease in $FEV_{0.1}$, all other significant effects of CAP exposure on pulmonary function observed in wildtype mice were invisible in mice deficient of IL-6R (Fig. 1B–G). In addition, Fig. S1 reveal that neither deficiency of IL-6R nor CAP exposure significantly influenced the body weight or food intake of these mice.

3.2. IL-6R deficiency reduces pulmonary inflammation induced by $PM_{2.5}$

Pulmonary inflammation may play a critical role for the development of pulmonary dysfunction, (Yao and Rahman, 2009) and $PM_{2.5}$ exposure is well known to induce pulmonary inflammation. (Arias-Pérez et al., 2020; Shamsollahi et al., 2021) Therefore we performed histological analysis on the lungs and quantitated their inflammatory levels through calculating the inflammatory score as described in Method. Fig. 2G shows that $PM_{2.5}$ exposure significantly increased the pulmonary inflammatory score in wildtype but not IL-6R-deficient mice. The increase in the pulmonary inflammatory score of wildtype mice following CAP exposure was attributable primarily to increases in pulmonary macrophage infiltration and alveolar distortion (Table 1 and Fig. 2F). To further document the effect of deficiency of IL-6R on $PM_{2.5}$ exposure-induced pulmonary inflammation, BALF cell differentiation analysis was also performed. Fig. 2A–B demonstrate that CAP exposure resulted in markedly increasing trends of total cells ($p = 0.06$), neutrophils ($p < 0.05$) and macrophages ($p = 0.06$) in the BALF of wildtype but not IL-6R-deficient mice. In contrast, neither CAP exposure nor deficiency of IL-6R markedly influenced the lymphocytes, eosinophils, and basophils of BALF in wildtype and IL-6R-deficient mice (Fig. 2B). To further document the effect of deficiency of IL-6R on $PM_{2.5}$ exposure-induced pulmonary inflammation, we assessed the pulmonary expressions of three classic inflammatory markers using real-time RT-PCR. Fig. 2C–E demonstrate that CAP exposure resulted in markedly increasing trends in pulmonary expressions of TNF-α, IL-6 and IL-1β mRNAs in wildtype but not IL-6R-deficient mice.

3.3. Effect of IL-6R deficiency on lung macrophage polarization

Macrophage polarization may massively determine the initiation, development and cessation of inflammation. (Hussell and Bell, 2014; Joshi et al., 2018) In addition, IL-6 signalling has been found to influence macrophage polarization. (Kraakman et al., 2015; Sanmarco et al., 2017) In order to test whether deficiency of IL-6R influences lung macrophage

polarization and subsequently pulmonary inflammation in response to $PM_{2.5}$, we analysed several macrophage polarization markers using real-time RT-PCR. Fig. 3A–D show that in wildtype control mice, CAP exposure significantly increased the pulmonary expression of TLR2 mRNA, a well-known M1 macrophage marker, (Allard et al., 2018; Hussell and Bell, 2014) and also resulted in increasing trends of pulmonary expressions of IL12, CD80 and CD66 mRNAs, three other well-known M1 macrophage markers. (Allard et al., 2018; Hussell and Bell, 2014) In contrast, $PM_{2.5}$ exposure did not considerably change the pulmonary expressions of these M1 macrophage markers in IL-6R-deficient mice (Fig. 3A–D). Furthermore, Fig. 3E–H reveal that CAP exposure resulted in marked decreasing trends in pulmonary expressions of TGF-β3, CCL22 and IL-13 mRNAs, three well-known M2 macrophage markers in wildtype mice, and that deficiency of IL-6R almost abolished these effects of CAP exposure.

3.4. IL-6R deficiency does not alleviate glucose intolerance and insulin resistance caused by $PM_{2.5}$ exposure

Chronic $PM_{2.5}$ exposure is shown to provoke marked glucose intolerance. (Chen et al., 2019; Wang et al., 2018) Pulmonary inflammation has been widely considered to be central for the glucose intolerance caused by $PM_{2.5}$ exposure. (Chen et al., 2019) To investigate the role of IL-6 signalling in promoting abnormal glucose homeostasis following $PM_{2.5}$ exposure, we additionally analyzed the effect of deficiency of IL-6R on $PM_{2.5}$ exposure-induced glucose intolerance and insulin resistance. IPGTT analysis illustrated that $PM_{2.5}$ exposure lead to significant glucose intolerance in wildtype mice, but deficiency of IL-6R, unexpectedly, did not appear to alleviate the glucose intolerance (Figs. 4A and 4B). In line with previous studies, (Hu et al., 2017) ITT analysis demonstrated that CAP exposure provoked significant insulin resistance in wildtype mice (Figs. 4C and 4D), supporting that $PM_{2.5}$ exposure-induced glucose intolerance may be accounted for primarily by insulin resistance. In line with the above mentioned IPGTT results and the mediation of $PM_{2.5}$ exposure-induced glucose intolerance by insulin resistance, deficiency of IL-6R did not markedly alleviate the insulin resistance induced by $PM_{2.5}$ exposure (Figs. 4C and 4D).

Hepatic insulin resistance has been found to account for the majority of whole-body insulin resistance following $PM_{2.5}$ exposure.(Hu et al., 2017) We thus assessed the hepatic insulin signalling of these CAP or FA-exposed mice. Fig. 4E–F reveal that CAP exposure resulted in a marked decreasing trend of insulin-induced AKT phosphorylation in both wildtype and IL-6R-deficient mice.

3.5. Hepatic effects of $PM_{2.5}$ exposure in IL-6R deficient and WT mice

Previous studies have shown that in parallel with hepatic insulin resistance, $PM_{2.5}$ exposure may also evoke a non-alcoholic steatohepatitis (NASH)-like pathology. (Tilg and Moschen, 2010; Xu et al., 2017) We, therefore, performed histological analyses on livers. H&E staining analysis showed that consistent with previous studies, (Tilg and Moschen, 2010; Xu et al., 2017) CAP exposure markedly increased the vacuole area, an indicator of lipid content, on hepatic sections of wildtype mice (Figs. 5A and 5B). Notably, deficiency of IL-6R did not appear to reduce this hepatic effect of CAP exposure (Figs. 5A and 5B). To verify the effect of deficiency of IL-6R on $PM_{2.5}$ exposure-induced NASH-like pathology,

Oil Red O staining analysis was conducted. Figs. 5A and 5D demonstrate that consistent with the vacuolation data, CAP exposure markedly increased the hepatic lipid content of wildtype mice, and deficiency of L-6R appeared to have no effect on this CAP exposure-induced increase in hepatic lipid content. Masson's trichrome staining analysis showed that neither CAP exposure nor deficiency of IL-6R significantly influenced the hepatic collagen contents (Figs. 5A and 5C).

3.6. $PM_{2.5}$ exposure increases adiposity in WT and IL-6R deficient mice

In addition to hepatic inflammation, $PM_{2.5}$ exposure has been shown to impair glucose homeostasis through promoting adipose dysfunction and inflammation.(Hu et al., 2017) Notably, Table 3 demonstrates that although $PM_{2.5}$ exposure did not significantly change the mouse body weight, it significantly increased the mass of epididymal, subcutaneous, and perirenal adipose tissues in both wildtype and IL-6R-deficient mice, supporting the notion that $PM_{2.5}$ exposure promotes adipose dysfunction and also suggesting that deficiency of IL-6 signalling does not influence the adipose effect of $PM_{2.5}$ exposure. Histological analysis on the epididymal adipose tissues revealed that the adipocyte sizes in both wildtype and IL-6R-deficient mice were significantly increased by CAP exposure (Figs. 6F and 6G), suggesting that $PM_{2.5}$ exposure increases mouse adiposity at least partly through induction of adipose hypertrophy. In line with previous studies, (Chen et al., 2018; Hu et al., 2017; Xu et al., 2011) mRNA expressions results showed that CAP exposure slightly upregulated the adipose expressions of TNF-α, CCL2 and SOCS3 in wildtype mice (Fig. 6A–E). Consistent with the adiposity result, IL-6R deficiency did not abolish the effect of $PM_{2.5}$ exposure on the expressions of TNF-α, CCL2 and SOCS3 (Fig. 6A–C).

4. Discussions

Inflammation is considered to be crucial in the pathogenesis due to $PM_{2.5}$ exposure. (EPA, 2020) It has been shown that inhaled $PM_{2.5}$ may directly provoke pronounced pulmonary inflammation. (EPA, 2020) Furthermore, the pulmonary inflammation is widely thought to be responsible for not only $PM_{2.5}$ exposure-induced pulmonary dysfunction but also various extra-pulmonary inflammations and subsequent dysfunctions (e.g., glucose intolerance and insulin resistance). (Rajagopalan et al., 2018) To test this notion, this study thoroughly investigated the effects of deficiency of IL-6R on $PM_{2.5}$ exposure-induced pulmonary and extra-pulmonary inflammations and dysfunctions. The main findings include that 1) deficiency of IL-6R significantly alleviated CAP exposure-induced pulmonary inflammation but not extra-pulmonary inflammation and dysfunction; 2) $PM_{2.5}$ exposure provoked both restrictive and obstructive lung diseases, and deficiency of IL-6R significantly alleviated these pulmonary dysfunctions; 3) IL-6R deficiency did not alleviate hepatic insulin resistance and NASH-like pathology caused by $PM_{2.5}$ exposure; 4) IL-6R deficiency did not significantly influence $PM_{2.5}$ exposure-induced adipose hypertrophy and inflammation.

From our perspective, the most important finding of this study is that deficiency of IL-6R ameliorates pulmonary but not extra-pulmonary inflammation and dysfunction. This finding strongly suggests that the development of extra-pulmonary inflammation and dysfunction is independent of pulmonary inflammation. This is in line with our previous

studies demonstrating that deletion of TNF/LT ameliorates pulmonary inflammation but not extra-pulmonary inflammation and dysfunction (Hu et al., 2017) and that short-term withdrawal from CAP exposure restores the extra-pulmonary inflammation and dysfunction but not pulmonary inflammation. (Ying et al., 2015) However, it should be noted that knockout of IL-6 was shown to block PM_{10} instillation-induced vascular dysfunction(Kido et al., 2011) and accelerated thrombosis (Mutlu et al., 2007). Therefore, it remains to be determined whether PM_{10} instillation model has different mechanism for the development of extra-pulmonary effects from that of CAP exposure model or the mechanism for $PM_{2.5}$ exposure provoking accelerated thrombosis and vascular dysfunction is different from that of insulin resistance and subsequent glucose intolerance. Albeit further study is clearly required, our studies provide considerable evidence against the current notion that pulmonary inflammation is central for the pathogenesis caused by $PM_{2.5}$ and thus, are expected to shift the conceptual framework for our understanding of the development of adverse extra-pulmonary effects following $PM_{2.5}$ exposure.

Although the present study clearly raises questions about the critical role of pulmonary inflammation for extra-pulmonary inflammation and dysfunction following $PM_{2.5}$ exposure, it strongly supports a crucial role of pulmonary inflammation on pulmonary dysfunction following $PM_{2.5}$ exposure. Along with our demonstration of decrease in CAP exposure-induced pulmonary inflammation by deficiency of IL-6R, as evidenced by the remarkable effects of deficiency of IL-6R on CAP exposure-induced pulmonary expressions of inflammatory markers, histological alterations, and increases in BALF macrophages and neutrophils (Fig. 2), we also clearly showed that deficiency of IL-6R abolished $PM_{2.5}$ exposure-induced decreases in FVC and C_{dyn} and increases in $FEV_{0.1}$/FVC, R_L, and R_E (Fig. 1). These present data are in line with the pathogenetic role of inflammation in the development of pulmonary dysfunction(Gan et al., 2004) and thus strongly support the crucial effect of pulmonary inflammation on pulmonary dysfunction following $PM_{2.5}$ exposure. However, given the emerging inflammation-independent role of IL-6 in the pathogenesis of various lung diseases, (Rincon and Irvin, 2012) further study is still needed to make sure whether pulmonary inflammation is a bystander or an active player for the pulmonary dysfunction after $PM_{2.5}$ exposure.

Notably, despite numerous epidemiological studies have shown the correlation between exposure to $PM_{2.5}$ and pulmonary dysfunction,(Da Silveira Fleck et al., 2021) the effect of $PM_{2.5}$ exposure on pulmonary function has hardly been investigated in animal models. The present data showing decreases in FVC and $FEV_{0.1}$ by CAP exposure in wildtype mice somehow are consistent with a most recent study showing a significant decrease in $FEF_{25–75\%}$ by 6-month exposure to PM_1 in a rat model.(Jheng et al., 2021) However, in contrast to the decrease in FEV_{20}/FVC shown by this most recent study, our study reveals that $PM_{2.5}$ exposure markedly increased $FEV_{0.1}$/FVC. An increase in $FEV_{0.1}$/FVC generally indicates restrictive lung disease.(D'Urzo et al., 2020) The development of restrictive lung disease following CAP exposure is also supported by the decrease in C_{dyn}. Furthermore, our histological analysis showed remarkable interstitial lung alteration, a common cause of restrictive lung disease,(D'Urzo et al., 2020) following CAP exposure. All these strongly suggest that exposure to $PM_{2.5}$ provokes restrictive lung disease in wildtype mice. Notably,

our result also showed that $PM_{2.5}$ exposure dramatically increased R_L and R_E, suggesting that $PM_{2.5}$ exposure evokes obstructive lung disease too.

Increasing studies have indicated that the role of IL-6 signalling in inflammation is context-dependent, which generally is pro-inflammatory but may be anti-inflammatory too.(Schumertl et al., 2021) Our demonstration of decrease in $PM_{2.5}$ exposure-induced pulmonary inflammation by deficiency of IL-6R is consistent with the frequently shown pro-inflammatory property of IL-6 signalling(Schumertl et al., 2021) and a previous study showing a critical role of IL-6 in pulmonary inflammation induced by PM_{10} instillation(Mutlu et al., 2007). Interestingly, another previous study revealed that deletion of IL-6 appeared to aggravate instillation of agriculture organic dust extract-induced pulmonary inflammation.(Wells et al., 2017) The discrepancy between the present study and this previous study has to be further investigated. In addition to the difference in exposure models, the different roles of mbIL-6R and sIL-6R in the inflammatory response may also account for this discrepancy.(Schumertl et al., 2021) While signalling by sIL-6R, also known as trans-signalling, is pro-inflammatory, signalling by mbIL-6R or classic signalling is anti--inflammatory.(Schumertl et al., 2021) Therefore, there is obviously an IL-6-independent mechanism for IL-6R regulating inflammatory responses, providing a potential explanation for this apparent discrepancy between the present study and the previous study.

In addition to the lack of significant effect on CAP exposure-induced insulin resistance, our results showed that IL-6R-deficienct versus control mice had significant insulin resistance (Fig. 4C–D). This is clearly consistent with a previous study demonstrating that deficiency of IL-6 resulted in insulin resistance,(Matthews et al., 2010) strongly supporting that IL-6R and IL-6 have comparable roles at least in regulation of glucose homeostasis. Except for IL-6, other cytokines such as TNF-α and IL-1β were also found to be involved in the development of abnormal glucose metabolism.(Akash et al., 2018)(Henriksbo et al., 2019) In the present study, the mRNA level of TNF-α in lung and white adipose tissue were both upregulated by $PM_{2.5}$ exposure (Fig. 2 and Fig. 6), thus the detailed role of TNF-α in the abnormal glucose homeostasis caused by $PM_{2.5}$ is worthy for further investigation. Furthermore, we(Chen et al., 2019) and others(Zheng et al., 2013) previously revealed that $PM_{2.5}$ exposure-induced abnormal glucose homeostasis was attributed primarily to hepatic inflammation and dysfunction. Therefore, it is particularly noteworthy that this study also showed that deficiency of IL-6R increased both basal and CAP exposure-induced hepatic inflammation (Fig. S2) but not adipose inflammation (Fig. 6). These data are consistent with tissue-specific deletion test showing that insulin resistance due to deficiency of IL-6R is accounted for primarily by deficiency of hepatic IL-6R(Whitham et al., 2019; Wunderlich et al., 2010). The present results obviously add to the evidence that hepatic inflammation and dysfunction is central for the abnormal glucose homeostasis induced by $PM_{2.5}$ exposure and independent of pulmonary inflammation, calling for reconsidering the putatively central role of pulmonary inflammation in the development of extra-pulmonary inflammation and dysfunction due to $PM_{2.5}$ exposure.

It’s well known that $PM_{2.5}$ is a complex mixture containing various chemicals including metal oxides, organic compounds and soluble salts, and numerous studies have demonstrated that the chemical composition of $PM_{2.5}$ may be crucial for its toxicity.(Seagrave et al.,

2006; Tao et al., 2021; Xu et al., 2021) Using multiple-pollutant models, Peng et al. found that among the major chemical components in $PM_{2.5}$, the concentrations of elemental carbon (EC) and organic carbon matter (OCM) were associated with the largest risks of emergency hospitalization for cardiovascular and respiratory diseases.(Peng et al., 2009) Our previous studies also revealed different action modes for different $PM_{2.5}$ fractions. While water-insoluble $PM_{2.5}$ compositions are responsible for pulmonary dysfunction and abnormal glucose homeostasis, the water-soluble $PM_{2.5}$ contribute to the change in gut microbiota.(Tao et al., 2021; Xu et al., 2021) However, based on the results in the present study, it's difficult to tell which components contribute most to the $PM_{2.5}$ exposure-induced adverse health effects or the role of IL-6 signaling in the toxicity of different $PM_{2.5}$ compositions, therefore additional studies are needed to fully understand the toxicological mechanisms underlying different chemical components in $PM_{2.5}$.

5. Conclusion

In summary, this study demonstrates distinct roles of IL-6 signalling in pulmonary and extra-pulmonary inflammations and dysfunctions following $PM_{2.5}$ exposure and thus provide evidence that may help reshape the conceptional framework for our understanding of development of various extra-pulmonary dysfunctions due to $PM_{2.5}$ exposure.

Supplementary Material

Refer to Web version on PubMed Central for supplementary material.

Funding

This work was funded by the National Key Research and Development Program of China (2019YFC1804503 to YX), the National Natural Science Foundation of China (Grant No. 82003414 to YX), and the National Institutes of Health (R01ES024516 and R01ES032290 to ZY).

Data availability

Data will be made available on request.

Abbreviations:

FA	filtered air
FVC	forced vital capacity
$PM_{2.5}$	ambient fine particles
VACES	versatile aerosol concentration enrichment system
CAP	concentrated ambient $PM_{2.5}$
AUC	Area under curve
XFS	X-ray fluorescence spectrometry
ITT	insulin tolerance test

IL-1β	interleukin-1 beta
IL-17A	interleukin-17A
IL-6	interleukin-6
IL-13	interleukin-13
IL-10	interleukin-10
IL-23	interleukin-23
IL-12	interleukin-12
IPGTT	intraperitoneal glucose tolerance test
PBS	phosphate buffer saline
TLR-2	Toll like receptor-2
TNF-α	tumor necrosis factor alpha
TGF-β	transforming growth factor-beta
TLR-4	Toll like receptor-4
CCL22	C-C chemokine ligand 22
CD80	the cluster of differentiation 80
CCL2	C-C chemokine ligand 2
CD86	the cluster of differentiation 86
SOCS3	suppressor of cytokine signaling-3
R_E	resistance of expiration
R_L	resistance of lung
C_{dyn}	respiratory dynamic compliance
$FEV_{0.1}$	forced expiratory volume in 0.1 s
Mac	macrophage
Lym	lymphocyte
Bas	basophil
Neu	neutrophil
Eos	eosinophil
Akt	protein kinase B
pAkt	phosphorylation of Akt

ANOVA analysis of variance

References

Akbari M, Hassan-Zadeh V, 2018. IL-6 signalling pathways and the development of type 2 diabetes. Inflammopharmacology 26, 685–698. [PubMed: 29508109]

Allard B, et al. , 2018. Alveolar macrophages in the resolution of inflammation, tissue repair, and tolerance to infection. Front Immunol. 9, 1777. [PubMed: 30108592]

Aparicio-Siegmund S, et al. , 2019. The IL-6-neutralizing sIL-6R-sgp130 buffer system is disturbed in patients with type 2 diabetes. Am. J. Physiol. Endocrinol. Metab. 317, E411–E420. [PubMed: 31237452]

Arias-Pérez RD, et al. , 2020. Inflammatory effects of particulate matter air pollution. Environ. Sci. Pollut. Res. 27, 42390–42404.

Brenachot X, et al. , 2017. Hepatic protein tyrosine phosphatase receptor gamma links obesity-induced inflammation to insulin resistance. Nat. Commun. 8, 1820. [PubMed: 29180649]

Chen M, et al. , 2018. Concentrated Ambient PM2.5-induced inflammation and endothelial dysfunction in a murine model of neural IKK2 deficiency. Environ. Health Perspect. 126, 027003. [PubMed: 29410383]

Chen S, et al. , 2019. Glucose homeostasis following diesel exhaust particulate matter exposure in a lung epithelial cell-specific IKK2-deficient mouse model. Environ. Health Perspect. 127, 57009. [PubMed: 31095431]

Da Silveira Fleck A, et al. , 2021. Environmental and occupational short-term exposure to airborne particles and FEV1 and FVC in healthy adults: a systematic review and meta-analysis. Int. J. Environ. Res. Public Health 18, 10571. [PubMed: 34682321]

D'Urzo KA, et al. , 2020. Variation among spirometry interpretation algorithms. Respir. Care 65, 1585–1590. [PubMed: 32291310]

EPA, Integrated Science Assessment (ISA) for Particulate Matter (Final Report, 2019). 2020.

Gan WQ, et al. , 2004. Association between chronic obstructive pulmonary disease and systemic inflammation: a systematic review and a meta-analysis. Thorax 59, 574–580. [PubMed: 15223864]

Giraldez MD, et al. , 2021. New insights into IL-6 family cytokines in metabolism, hepatology and gastroenterology. Nat. Rev. Gastroenterol. Hepatol. 18, 787–803. [PubMed: 34211157]

Hamanaka RB, Mutlu GM, 2018. Particulate matter air pollution: effects on the cardiovascular system. Front Endocrinol. (Lausanne) 9, 680. [PubMed: 30505291]

Henriksbo BD, et al. , 2019. Statins promote interleukin-1beta-dependent adipocyte insulin resistance through lower prenylation, not cholesterol. Diabetes 68, 1441–1448. [PubMed: 31010959]

Hu Z, et al. , 2017. Inactivation of TNF/LT locus alters mouse metabolic response to concentrated ambient PM2.5. Toxicology 390, 100–108. [PubMed: 28917655]

Huang T, et al. , 2022. Adipocyte-derived kynurenine promotes obesity and insulin resistance by activating the AhR/STAT3/IL-6 signaling. Nat. Commun. 13, 3489. [PubMed: 35715443]

Hunter CA, Jones SA, 2015. IL-6 as a keystone cytokine in health and disease. Nat. Immunol. 16, 448–457. [PubMed: 25898198]

Hussell T, Bell TJ, 2014. Alveolar macrophages: plasticity in a tissue-specific context. Nat. Rev. Immunol. 14, 81–93. [PubMed: 24445666]

Jheng Y-T, et al. , 2021. Prolonged exposure to traffic-related particulate matter and gaseous pollutants implicate distinct molecular mechanisms of lung injury in rats. Part. Fibre Toxicol. 18.

Joshi N, et al. , 2018. Alveolar Macrophages. Cell Immunol. 330, 86–90. [PubMed: 29370889]

Karagulian F, et al. , 2015. Contributions to cities' ambient particulate matter (PM): A systematic review of local source contributions at global level. Atmos. Environ. 120, 475–483.

Kido T, et al. , 2011. Particulate matter induces translocation of il-6 from the lung to the systemic circulation. Am. J. Respir. Cell Mol. Biol. 44, 197–204. [PubMed: 20378751]

Kraakman MJ, et al. , 2015. Blocking IL-6 trans-signaling prevents high-fat diet-induced adipose tissue macrophage recruitment but does not improve insulin resistance. Cell Metab. 21, 403–416. [PubMed: 25738456]

Marasco MR, et al. , 2018. Interleukin-6 reduces beta-cell oxidative stress by linking autophagy with the antioxidant response. Diabetes 67, 1576–1588. [PubMed: 29784660]

Matthews VB, et al. , 2010. Interleukin-6-deficient mice develop hepatic inflammation and systemic insulin resistance. Diabetologia 53, 2431–2441. [PubMed: 20697689]

McFarland-Mancini MM, et al. , 2010. Differences in wound healing in mice with deficiency of IL-6 versus IL-6 receptor. J. Immunol. 184, 7219–7228. [PubMed: 20483735]

Mutlu GM, et al. , 2007. Ambient particulate matter accelerates coagulation via an IL-6–dependent pathway. J. Clin. Investig. 117, 2952–2961. [PubMed: 17885684]

Narazaki M, Kishimoto T, 2018. The Two-Faced Cytokine IL-6 in Host Defense and Diseases. Int J. Mol. Sci. 19.

Peng RD, et al. , 2009. Emergency admissions for cardiovascular and respiratory diseases and the chemical composition of fine particle air pollution. Environ. Health Perspect. 117, 957–963. [PubMed: 19590690]

Rajagopalan S, et al. , 2018. Air pollution and cardiovascular disease: JACC state-of-the-art review. J. Am. Coll. Cardiol. 72, 2054–2070. [PubMed: 30336830]

Rehman K, et al. , 2017. Role of interleukin-6 in development of insulin resistance and type 2 diabetes mellitus. Crit. Rev. Eukaryot. Gene Expr. 27, 229–236. [PubMed: 29199608]

Rincon M, Irvin CG, 2012. Role of IL-6 in asthma and other inflammatory pulmonary diseases. Int J. Biol. Sci. 8, 1281–1290. [PubMed: 23136556]

Sanmarco LM, et al. , 2017. IL-6 promotes M2 macrophage polarization by modulating purinergic signaling and regulates the lethal release of nitric oxide during Trypanosoma cruzi infection. Biochim Biophys. Acta Mol. Basis Dis. 1863, 857–869. [PubMed: 28087471]

Schumertl T, et al. , 2021. Function and proteolytic generation of the soluble interleukin-6 receptor in health and disease. Biochim Biophys. Acta Mol. Cell Res 1869, 119143. [PubMed: 34626681]

Seagrave J, et al. , 2006. Lung toxicity of ambient particulate matter from southeastern U.S. sites with different contributing sources: relationships between composition and effects. Environ. Health Perspect. 114, 1387–1393. [PubMed: 16966093]

Shamsollahi HR, et al. , 2021. Particulates induced lung inflammation and its consequences in the development of restrictive and obstructive lung diseases: a systematic review. Environ. Sci. Pollut. Res. 28, 25035–25050.

Tao S, et al. , 2021. Exposure to different fractions of diesel exhaust PM2.5 induces different levels of pulmonary inflammation and acute phase response. Ecotoxicol. Environ. Saf. 210, 111871. [PubMed: 33422840]

Tilg H, Moschen AR, 2010. Evolution of inflammation in nonalcoholic fatty liver disease: the multiple parallel hits hypothesis. Hepatology 52, 1836–1846. [PubMed: 21038418]

Wang W, et al. , 2018. Exposure to concentrated ambient PM2.5 alters the composition of gut microbiota in a murine model. Part Fibre Toxicol. 15, 17. [PubMed: 29665823]

Wells A, et al. , 2017. Systemic IL-6 effector response in mediating systemic bone loss following inhalation of organic dust. J. Interferon Cytokine Res. 37, 9–19. [PubMed: 27875664]

Whitham M, et al. , 2019. Adipocyte-specific deletion of IL-6 does not attenuate obesity-induced weight gain or glucose intolerance in mice. Am. J. Physiol. Endocrinol. Metab. 317, E597–E604. [PubMed: 31386565]

Wunderlich FT, et al. , 2010. Interleukin-6 signaling in liver-parenchymal cells suppresses hepatic inflammation and improves systemic insulin action. Cell Metab. 12, 237–249. [PubMed: 20816090]

Xiang M, et al. , 2019. Direct in vivo application of induced pluripotent stem cells is feasible and can be safe. Theranostics 9, 290–310. [PubMed: 30662568]

Xie Y, et al. , 2015. Daily Estimation of Ground-Level PM2.5 Concentrations over Beijing Using 3 km Resolution MODIS AOD. Environ. Sci. Technol. 49, 12280–12288. [PubMed: 26310776]

Xu J, et al. , 2017. Airborne PM2.5-Induced Hepatic Insulin Resistance by Nrf2/JNK-Mediated Signaling Pathway. Int J. Environ. Res Public Health 14.

Xu X, et al. , 2011. Long-term exposure to ambient fine particulate pollution induces insulin resistance and mitochondrial alteration in adipose tissue. Toxicol. Sci. 124, 88–98. [PubMed: 21873646]

Xu Y, et al. , 2019. Metabolomics analysis of a mouse model for chronic exposure to ambient PM2.5. Environ. Pollut. 247, 953–963. [PubMed: 30823350]

Xu Y, et al. , 2021. Differential roles of water-insoluble and water-soluble fractions of diesel exhaust particles in the development of adverse health effects due to chronic instillation of diesel exhaust particles. Chem. Res. Toxicol. 34, 2450–2459. [PubMed: 34780166]

Yao H, Rahman I, 2009. Current concepts on the role of inflammation in COPD and lung cancer. Curr. Opin. Pharmacol. 9, 375–383. [PubMed: 19615942]

Ying Z, et al. , 2015. Exposure to concentrated ambient particulate matter induces reversible increase of heart weight in spontaneously hypertensive rats. Part Fibre Toxicol. 12, 15. [PubMed: 26108756]

Yue H, et al. , 2017. Maternal Exposure of BALB/c Mice to Indoor NO2 and Allergic Asthma Syndrome in Offspring at Adulthood with Evaluation of DNA Methylation Associated Th2 Polarization. Environ. Health Perspect. 125, 097011. [PubMed: 28935613]

Zhang L, et al. , 2020. Mining sequential patterns of PM2.5 pollution between 338 cities in China. J. Environ. Manag. 262, 110341.

Zheng Y, et al. , 2020. Potential crosstalk between liver and extra-liver organs in mouse models of acute liver injury. Int J. Biol. Sci. 16, 1166–1179. [PubMed: 32174792]

Zheng Z, et al. , 2013. Exposure to ambient particulate matter induces a NASH-like phenotype and impairs hepatic glucose metabolism in an animal model. J. Hepatol. 58, 148–154. [PubMed: 22902548]

Zhou S, et al. , 2020. Ovarian dysfunction induced by chronic whole-body PM2.5 exposure. Small 16, 2000845.

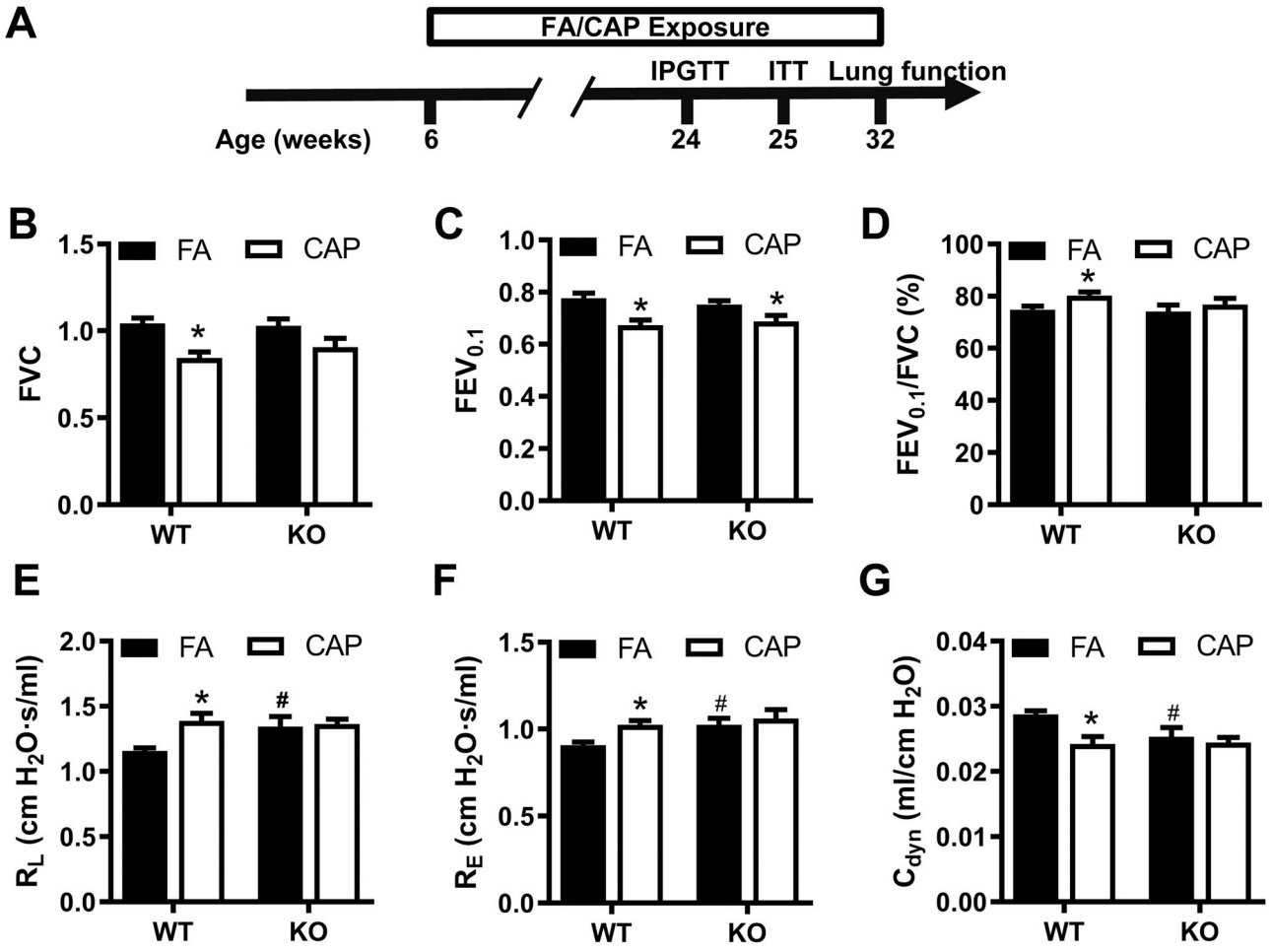

Fig. 1. IL-6R deficiency alleviates pulmonary dysfunction induced by $PM_{2.5}$ exposure.

Male mice (C57Bl/6 J) were exposed to FA or CAP for 26 weeks and then subjected to lung function test. A, the experimental scheme. B-G, the pulmonary function estimators FVC (A), $FEV_{0.1}$ (B), $FEV_{0.1}$/FVC (C), R_L (D), R_E (E), C_{dyn} (F) of the CAP/FA exposed mice. Data are represented as mean±SEM, n = 11–12/group, #$p < 0.05$ versus WT, * $p < 0.05$ versus FA, two-way ANOVA. KO: IL-6R knock out mice (IL-$6R^{-/-}$), WT: littermate control wildtype mice (IL-$6R^{+/+}$).

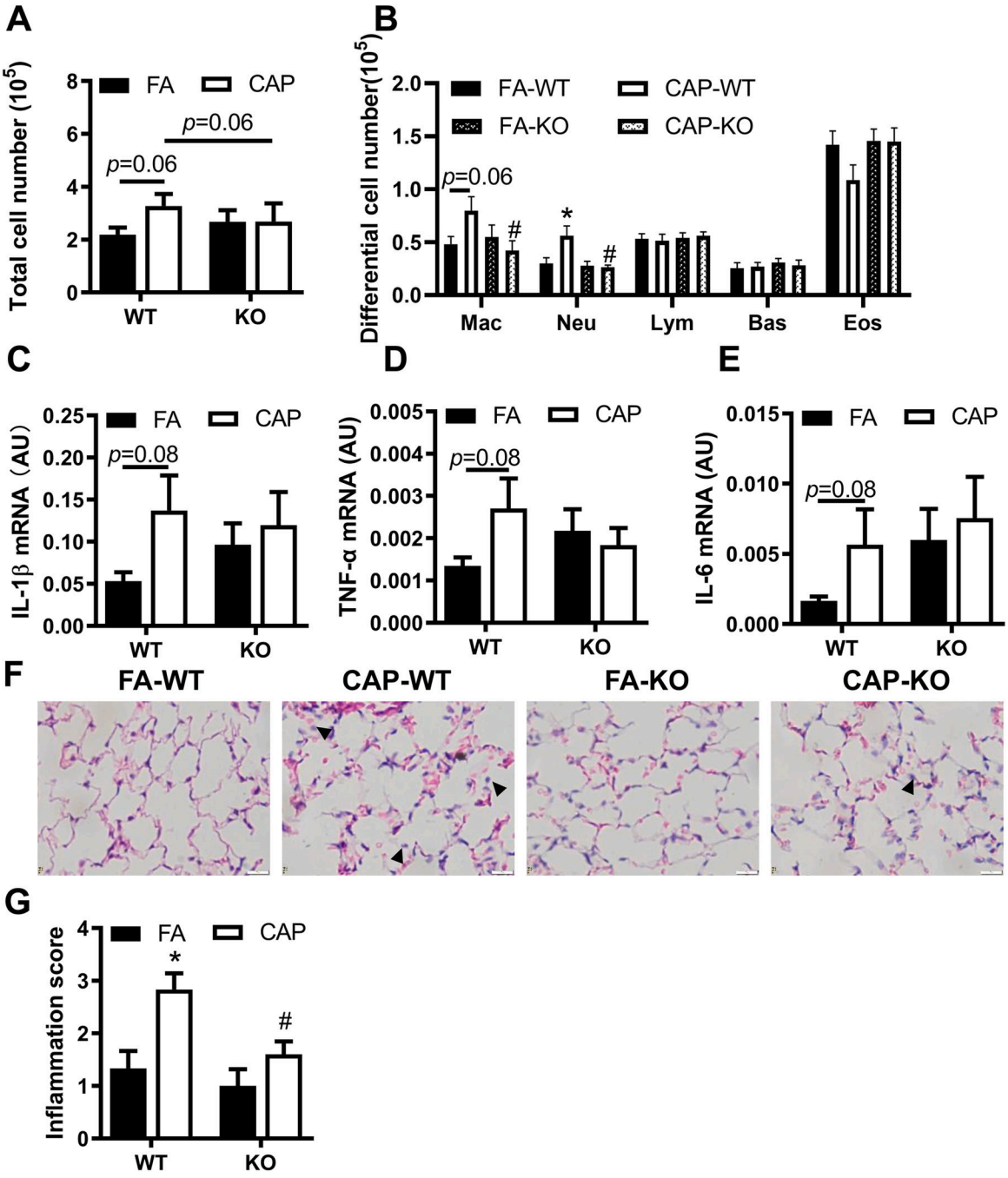

Fig. 2. IL-6R deficiency reduces $PM_{2.5}$ exposure-induced pulmonary inflammation.

A-B, the total cell number (A) and differential cell numbers (B) in BALF. Mac: macrophages/monocytes; Neu: neutrophils; Lym: lymphocytes; Bas: basophils; Eos: eosinophils. n = 11–12/group, #$p < 0.05$ versus WT, * $p < 0.05$ versus FA, two-way ANOVA. C-E, the mRNA levels of inflammatory cytokines IL-1β (C), TNF-α (D) and IL-6 (E) in lung. n = 5–6/group, #$p < 0.05$ versus WT, * $p < 0.05$ versus FA, two-way ANOVA. F, the representative images of H&E staining analysis of lung. Black arrow: macrophage infiltration. G, the inflammation score based on H&E images. Data are represented as

mean±SEM, n = 5/group, #$p < 0.05$ versus WT, * $p < 0.05$ versus FA, two-way ANOVA. KO: IL-6R knock out mice (IL-6R$^{-/-}$), WT: littermate control wildtype mice (IL-6R$^{+/+}$).

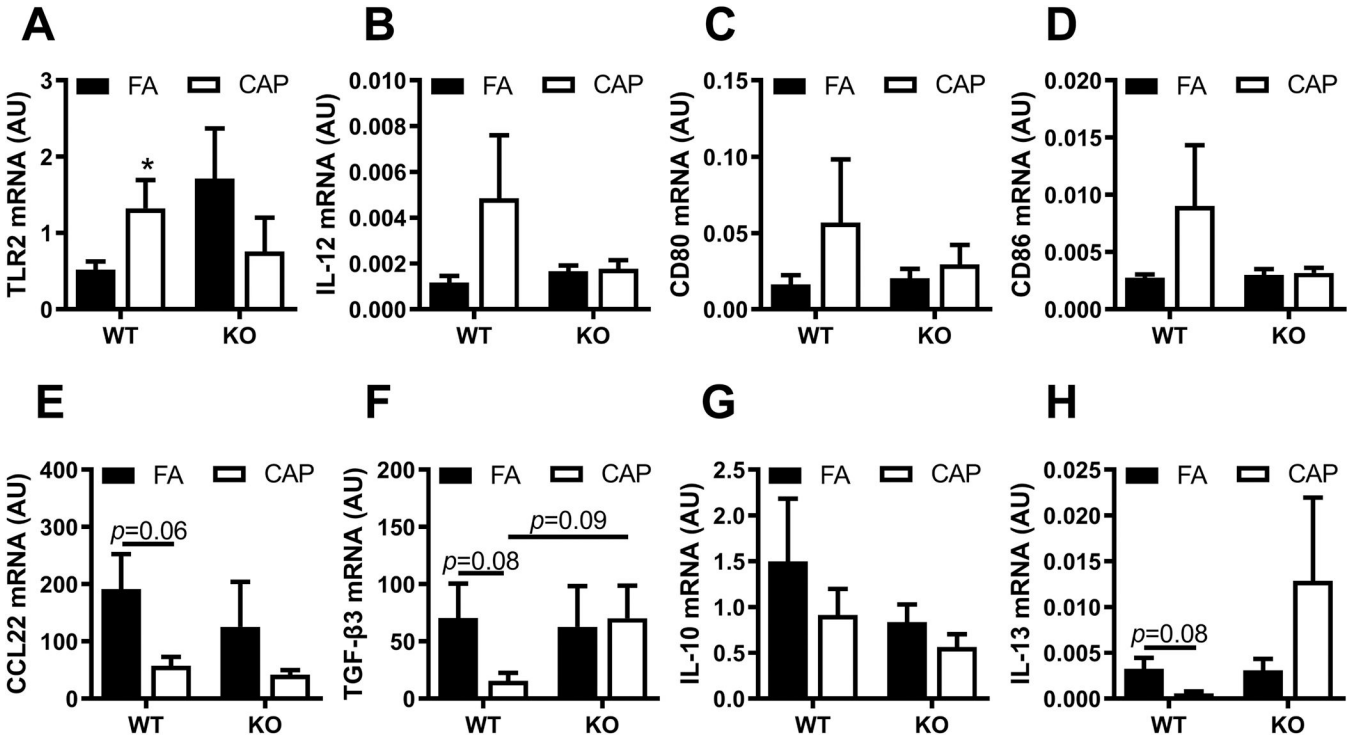

Fig. 3. Effect of IL-6R deficiency on lung macrophage polarization.

A-D, mRNA levels of M1 macrophage biomarkers TLR2 (A), IL-12 (B), CD80 (C) and CD86 (D) in lungs of CAP/FA exposed mice. E-H, mRNA levels of M2 macrophage biomarkers CCL22 (E), TGF-β3 (F), IL-10 (G) and IL-13 (H) in lungs of CAP/FA exposed mice. Data are represented as mean±SEM, n = 5–6/group, #$p < 0.05$ versus WT, * $p < 0.05$ versus FA, two-way ANOVA. KO: IL-6R knock out mice (IL-6R$^{-/-}$), WT: littermate control wildtype mice (IL-6R$^{+/+}$).

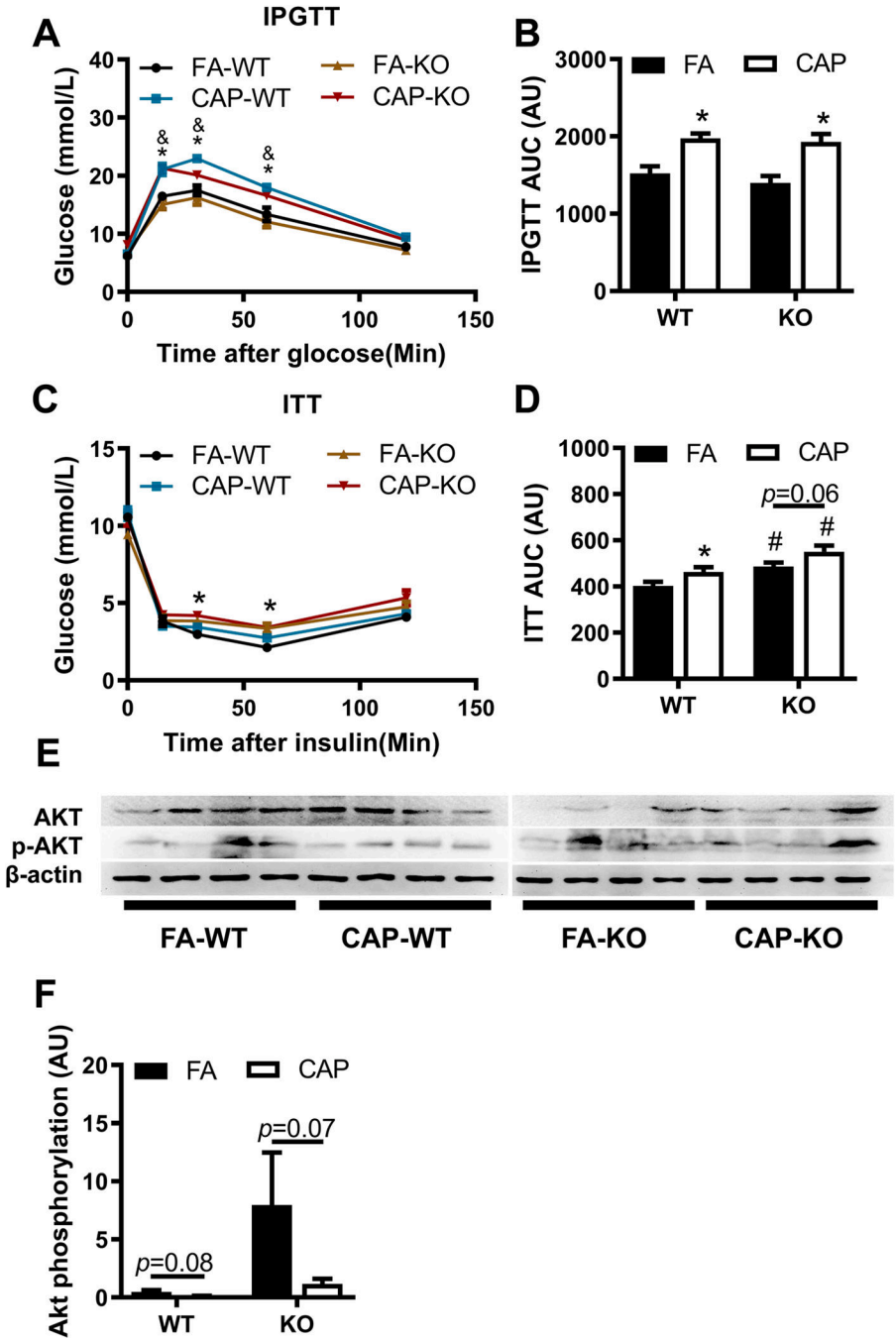

Fig. 4. IL-6R deficiency does not alleviate $PM_{2.5}$ exposure-induced insulin resistance or glucose intolerance.

A, the response curve of IPGTT after 18 weeks of FA/CAP exposure. n = 11–12/group, * $p < 0.05$ for CAP-WT versus FA-WT, &$p < 0.05$ for CAP-KO versus FA-KO, two-way ANOVA. B, the AUC of IPGTT. n = 11–12/group, * $p < 0.05$ versus FA, two-way ANOVA. C, the response curve of ITT. n = 11–12/group, * $p < 0.05$ for CAP-WT versus FA-WT, two-way ANOVA. D, the AUC of ITT. n = 11–12/group, #$p < 0.05$ versus WT, * $p <$ 0.05 versus FA, two-way ANOVA. E-F, Mice were fasted overnight and intraperitoneally injected with insulin (10 U/kg of body weight) 20 min before sacrifice. The insulin-induced

Akt phosphorylation levels in liver were assessed by western blot. Data are represented as mean±SEM, n = 11–12/group, #$p < 0.05$ versus WT, * $p < 0.05$ versus FA, two-way ANOVA. KO: IL-6R knock out mice (IL-6R$^{-/-}$), WT: littermate control wildtype mice (IL-6R$^{+/+}$).

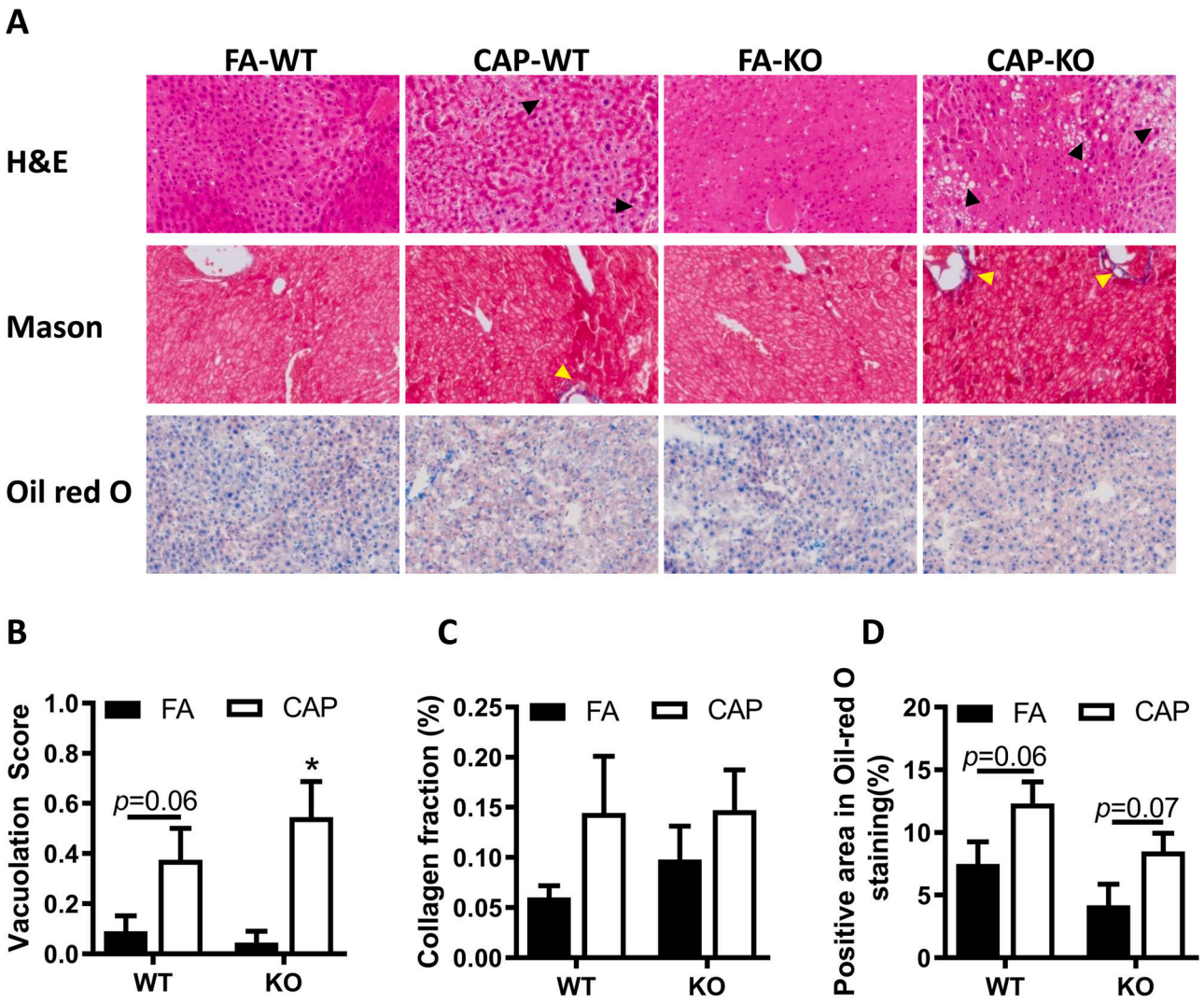

Fig. 5. Hepatic effects of $PM_{2.5}$ exposure in IL-6R deficient and WT mice.

A, the representative H&E, Mason's trichrome and Oil Red O staining images of liver from FA/CAP exposed mice. Black arrow: cell vacuolation; yellow arrow: collagen fiber. B, the quantitation of vacuolation score based on H&E images. C, the quantitation of collagen volume fraction based on Mason's trichrome staining images. D, the quantitation of positive area in Oil Red O staining images. Data are represented as mean±SEM, n = 11–12/group, #$p < 0.05$ versus WT, * $p < 0.05$ versus FA, two-way ANOVA. KO: IL-6R knock out mice (IL-$6R^{-/-}$), WT: littermate control wildtype mice (IL-$6R^{+/+}$).

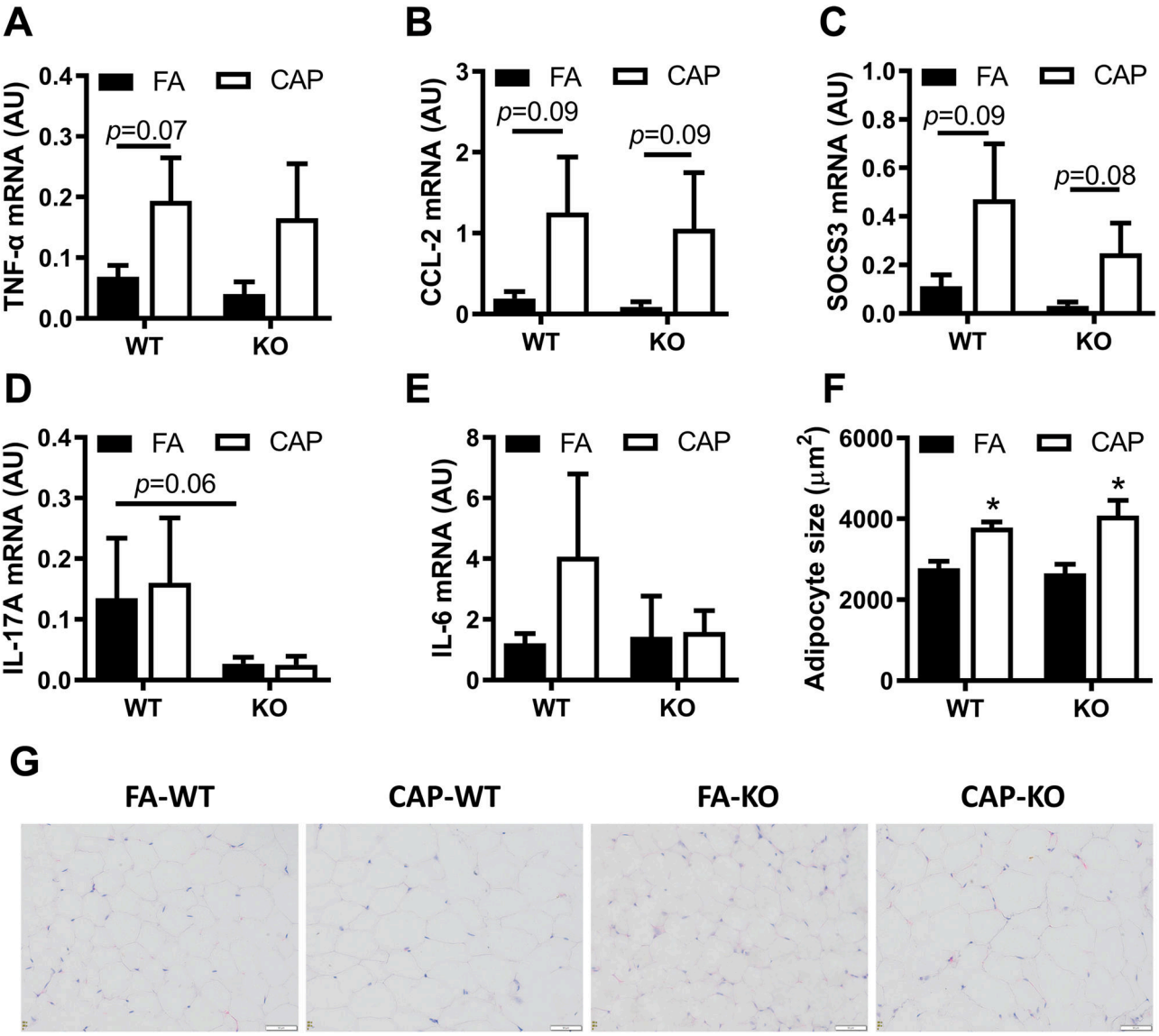

Fig. 6. $PM_{2.5}$ exposure increases adiposity in WT and IL-6R deficient mice.

A-E, mRNA levels of pro-inflammatory cytokines in epididymal adipose tissue of FA/CAP exposed mice. F-G, the representative H&E images (G) and adipocyte size (F) quantified based on the H&E images. Data are represented as mean±SEM, n = 11–12/group, #$p < 0.05$ versus WT, * $p < 0.05$ versus FA, two-way ANOVA. KO: IL-6R knock out mice (IL-$6R^{-/-}$), WT: littermate control wildtype mice (IL-$6R^{+/+}$).

Table 1

The scoring system and results of pulmonary inflammation.

	Scoring standard	FA-WT	CAP-WT	FA-KO	CAP-KO
Oedema	Presence,1; absence,0;	0.00 ± 0.00	0.00 ± 0.00	0.00 ± 0.00	0.00 ± 0.00
Hyperaemia	Presence,1; absence,0;	0.83 ± 0.37	1.00 ± 0.00	0.80 ± 0.40	1.00 ± 0.00
Haemorrhage	Presence,1; absence,0;	0.33 ± 0.47	0.67 ± 0.47	0.20 ± 0.40	0.40 ± 0.49
Interalveolar thickness	Presence of every 10% area= 1	0.17 ± 0.37	0.17 ± 0.37	0.00 ± 0.00	0.00 ± 0.00
Macrophage infiltration	Presence of every 10% area= 1	0.00 ± 0.00	0.50 ± 0.50 *	0.00 ± 0.00	0.20 ± 0.40
Alveolar distortion	Presence of every 10% area= 1	0.00 ± 0.00	0.50 ± 0.50 *	0.00 ± 0.00	0.00 ± 0.00#

Data are represented as mean ± SEM (n = 5/group)

* $p < 0.05$ vs FA

# $p < 0.05$ vs WT, two-way ANOVA

KO: IL-6R knock out mice (IL-6R$^{-/-}$), WT: littermate control wildtype mice (IL-6R$^{+/+}$)

Table 2

The elemental compositions of $PM_{2.5}$ analyzed by XRF.

Elements	FA (μg/m^3)	CAP (μg/m^3)	Ambient (μg/m^3)
Cr	*ND*	*ND*	*ND*
As	*ND*	*ND*	*ND*
Si	0.17 ± 0.01	1.28 ± 0.24	0.23 ± 0.07
Se	*ND*	*ND*	*ND*
S	0.41 ± 0.04	9.43 ± 4.05	1.56 ± 1.19
P	*ND*	0.04 ± 0.05	*ND*
V	*ND*	0.05 ± 0.00	*ND*
Ca	*ND*	0.66 ± 0.36	*ND*
Ti	*ND*	0.05 ± 0.00	*ND*
Na	*ND*	0.63 ± 0.62	*ND*
Ba	*ND*	*ND*	*ND*
Sc	*ND*	*ND*	*ND*
Co	*ND*	*ND*	*ND*
K	0.11 ± 0.03	1.95 ± 0.99	0.31 ± 0.22
Fe	*ND*	1.57 ± 0.19	0.25 ± 0.00
Pb	*ND*	0.12 ± 0.00	*ND*
Cu	*ND*	0.40 ± 0.23	0.06 ± 0.01
Al	*ND*	0.22 ± 0.12	0.01 ± 0.00
Zn	0.03 ± 0.01	0.85 ± 0.40	0.06 ± 0.03
Sn	0.20 ± 0.01	0.21 ± 0.03	0.18 ± 0.00
Mn	*ND*	0.17 ± 0.03	*ND*
Mg	*ND*	0.04 ± 0.00	*ND*
Cd	*ND*	*ND*	*ND*
Ni	0.02 ± 0.00	1.35 ± 0.50	0.04 ± 0.00

Data are represented as mean ± SEM (n = 10–15/group), ND: Non-detectable

Table 3

Organ weights of mice after FA/CAP exposure.

	WT			KO		
	FA	**CAP**	***p-value***	**FA**	**CAP**	***p-value***
Body length(cm)	10.28 ± 0.31	10.34 ± 0.52	0.75	10.43 ± 0.35	10.35 ± 0.31	0.65
Brain (g)	0.46 ± 0.02	0.47 ± 0.02	0.32	0.47 ± 0.02	0.46 ± 0.02	0.25
Brown adipose tissue (g)	0.21 ± 0.06	0.24 ± 0.04	0.18	0.21 ± 0.04	0.22 ± 0.03	0.52
Heart (g)	0.15 ± 0.03	0.16 ± 0.03	0.51	0.16 ± 0.03	0.16 ± 0.03	0.97
Lung (g)	0.05 ± 0.00	0.05 ± 0.01	0.75	0.05 ± 0.01	0.05 ± 0.01	0.36
Liver (g)	1.23 ± 0.15	1.31 ± 0.16	0.22	1.15 ± 0.13	1.26 ± 0.22	0.20
Spleen (g)	0.08 ± 0.02	0.08 ± 0.01	0.78	0.07 ± 0.01	0.06 ± 0.01	0.08
Pancreas (g)	0.18 ± 0.04	0.20 ± 0.04	0.31	0.21 ± 0.04	0.17 ± 0.05	0.08
Kidney (g)	0.39 ± 0.03	0.40 ± 0.04	0.60	0.40 ± 0.04	0.37 ± 0.04	0.13
Perirenal fat (g)	0.38 ± 0.17	0.52 ± 0.13	0.05 *	0.27 ± 0.13	0.47 ± 0.19	0.02 *
Subcutaneous fat (g)	0.40 ± 0.16	0.55 ± 0.13	0.03 *	0.32 ± 0.11	0.56 ± 0.25	0.02 *
Skeletal muscle (g)	0.34 ± 0.02	0.35 ± 0.03	0.16	0.35 ± 0.02	0.34 ± 0.02	0.74
Testis (g)	0.18 ± 0.02	0.19 ± 0.01	0.17	0.18 ± 0.02	0.17 ± 0.03	0.45
Epididymis (g)	0.08 ± 0.01	0.08 ± 0.01	0.76	0.08 ± 0.01	0.08 ± 0.01	0.64
Epididymal adipose tissue (g)	1.18 ± 0.42	1.58 ± 0.37	0.03 *	0.84 ± 0.35	1.41 ± 0.54	0.01 *

Data are represented as mean ± SEM (n = 11–12/group)

* $p<0.05$ vs FA

\# $p<0.05$ vs WT, two-way ANOVA

KO: IL-6R knock out mice (IL-6R$^{-/-}$), WT: littermate control wildtype mice (IL-6R$^{+/+}$)